Contribution of the Mitochondrial Compartment to the Optical Properties of the Rat Liver: A Theoretical and Practical Approach

B. Beauvoit, T. Kitai, and B. Chance
Department of Biochemistry and Biophysics, University of Pennsylvania, Philadelphia, Pennsylvania 19104 USA

ABSTRACT The purpose of this work was to analyze the contribution of the mitochondria to the optical properties, i.e., light absorption and scattering, of the blood-free rat liver. Firstly, a theoretical model of the reduced scattering coefficient of the liver was performed by using the Mie theory, the Rayleigh-Debye-Gans approximation, and the electron microscopy descriptions of the liver ultrastructure. Compared with the hepatocyte volume, the nucleus and the peroxisomes, the mitochondria compartment, accounting for 22% of the liver cell volume, seemed to be the predominant factor for the light scattering of the liver. Second, by using time-resolved spectroscopy and a sample substitution method, we have measured the absorption and reduced scattering coefficients of blood-free perfused rat livers, isolated hepatocyte suspensions, and isolated mitochondria suspensions. A subsequent extrapolation of the isolated mitochondria data to the in vivo mitochondrial content and a comparison with the whole liver measurements lead to the following conclusions: 1) the mitochondria account for about 50% of the liver absorption coefficient at 780 nm (μ_a = 0.25 cm^{-1} extrapolated from isolated mitochondria vs. 0.53 ± 0.05 cm^{-1} measured for the liver); and 2) the mitochondrial compartment is the primary factor for the light scattering in the rat liver (μ_s' = 15.5 cm^{-1} extrapolated from the isolated mitochondria versus 15.9 ± 2.4 cm^{-1} measured for the liver), demonstrating the relevancy of our preliminary theoretical study.

INTRODUCTION

Near-infrared (NIR) time-resolved spectroscopy (TRS) is a useful noninvasive means to study the optical properties (absorption and scattering) of tissue (Patterson et al., 1989; Wilson et al., 1992). Based on the theory of photon transport in a highly scattering medium (conditions where the Beer-Lambert law vanishes), this technique allows the independent determination of two macroscopic optical parameters: absorption (μ_a) and reduced scattering coefficients (μ_s'). The total light absorption is the sum of the absorption due to endogenous chromophores. For instance, in the NIR spectral window, these compounds consists of hemoglobin, myoglobin and cytochrome aa_3, in both reduced and oxygenated state, and water as well. It is now well established that the measurement of the absorption coefficient, at different wavelengths, can be used to calculate the in situ hemoglobin oxygenation (Chance et al., 1988a, b; Sevick et al., 1991). Elastic light scattering by soft tissues is associated with the microscopic heterogeneity in the tissue dielectric constant. The detailed dependence of scattering on tissue architecture and intracellular composition is not well understood. Theoretical models for scattering such as Mie theory or the Rayleigh-Debye-Gans (RDG) approximation depend on three characteristic parameters of the particle, namely the shape, the particle size to wavelength ratio, and the refractive index (Van de Hulst, 1957; Kerker, 1969; Ishimaru, 1978; Bohren and Huffman, 1983). Single scattering experiments that measured the angular distribution of scattered light intensity on bacterial (Cross and Latimer, 1972) and mammalian (Reynolds et al., 1976; Sloot et al., 1988; Steinke and Shepherd, 1988; Frank et al., 1989) cell suspensions have supported the validity of these approximations.

A recent approach, combining the determinations of the μ_s' of yeast cell suspensions by TRS and Mie theory calculations clearly demonstrated that the cell size is the primary factor affecting the light scattering regardless to the differentiation status of the mitochondria (Beauvoit et al., 1993). These results could be interpreted in two ways: mitochondria per se do not contribute to the light scattering, or the total volume of the mitochondrial compartment and/or the number of mitochondria inside the yeast cell is small. Electron microscopy and fluorescence staining techniques have demonstrated that the number, form, and volume of mitochondria are closely related to the life cycle and physiological state of the yeast cell (Hoffman and Avers, 1973; Stevens, 1981). For example, the mitochondrial compartment morphology varies from a giant branched mitochondrion (Hoffman and Avers, 1973; Miyakawa et al., 1984) to about 50 mitochondria particles per yeast cell (Lloyd, 1974; Stevens, 1981; Miyakawa et al., 1984). Moreover, the volume fraction varies from 3 to 12% of the total cell volume (Lloyd, 1974; Stevens, 1981).

The mitochondrial compartment of mammalian cells is more disperse than microorganism mitochondria. As a matter of fact, fluorescence staining of various cultured mammalian cells showed a filamentous structure of the mitochondrion (Johnson et al., 1980; for review see Chen, 1989) and

Received for publication 24 January 1994 and in final form 21 September 1994.

Address reprint requests to Dr. Britton Chance, Johnson Research Foundation, D501 Richards Building, Department of Biochemistry and Biophysics, University of Pennsylvania, Philadelphia, PA 19104. Tel.: 215-898-4342; Fax: 215-898-1806.

Abbreviations used: NIR, near infrared; TRS, time-resolved spectroscopy; μ_a and μ_s', absorption and reduced scattering coefficients (Napierian log base), respectively; σ_a and σ_{tr}, absorption and transport cross-sections, respectively.

0006-3495/94/12/2501/10 $2.00

recently, a "string of beads" appearance has been demonstrated (Smiley et al., 1991). In contrast to other mammalian cells, the hepatocytes exhibit a polydisperse fluorescent staining of the mitochondrial compartment (Lemasters et al., 1987; Reber et al., 1990). Indeed, the hepatocyte mitochondria and the peroxisomes can be observed as spherical particles by three-dimensional electron microscopy (Furuta et al., 1992). It should be noted that this disperse or granular mitochondrial compartment can be transformed in a giant mitochondrion under pathological conditions (for review see Tandler and Hoppel, 1986). Moreover, the morphometric and biochemical analysis of the rat liver (Loud, 1968;Weibel et al., 1969; Blouin et al., 1977; Jakovcic et al., 1978) and the isolated hepatocytes (Pfaller et al., 1993; Halestrap, 1989) have demonstrated that the mitochondrial compartment is the most prominent cellular compartment, with a volume fraction of about 19–28% of the total cell volume.

The aim of the present study is to determine the relative importance of the mitochondria content of the liver cell toward the light scattering and absorption (at 780 nm) of the whole organ. Two independent ways were investigated. One was theoretical calculations based on two mathematical models: Mie theory and Rayleigh-Debye-Gans (RDG) approximation. These calculations can predict the respective contribution of the hepatocyte total volume and the three major subcellular compartments (i.e., the nucleus, the mitochondria and the peroxisomes) to the global reduced scattering coefficient of the liver. The other was an experimental approach using TRS and a substitution method. This part measures the μ_a and μ_s' of the blood-free perfused liver and compares with the results obtained in vitro on isolated hepatocytes and isolated mitochondria.

MATERIALS AND METHODS

Liver perfusion

Male Sprague-Dawley rats (250–300 g) were fed ad libitum before experiment. Rats were anesthetized by intraperitoneal injection of pentobarbital (50 mg/kg body mass) and the liver was perfused at a flow rate of 30 ml/min (~2.5 ml/min/g liver mass), with a Hanks/HEPES buffer (pH 7.4, 37°C) composed of 137 mM NaCl, 5.4 mM KCl, 4.2 mM $NaHCO_3$, 1.2 mM NaH_2PO_4, 1.25 mM $CaCl_2$, 0.4 mM $MgSO_4$, 0.5 mM $MgCl_2$, 10 mM HEPES, supplemented with 5 mM glucose. The liver was removed from the carcass and placed in a plastic bag for TRS measurements. Perfusion flow was stopped just before taking measurement and the liver samples were stored on ice between two TRS measurements. It is assumed that the perfusion cessation does not induce any change in optical properties during the short period of the TRS measurements (1–5 min).

Hepatocyte isolation

Rat liver parenchymal cells were isolated by using the two-step procedure as described in Berry et al. (1991). First, the liver was washed out for 10 min with a Hanks/HEPES solution (pH 7.4, 37°C) without calcium and magnesium and containing 0.5 mM EGTA. Then, liver was perfused for 15 min with a Hanks/HEPES solution containing 3.8 mM $CaCl_2$, 0.05% collagenase (Sigma Chemical Co., St. Louis, MO; type I-A) and 0.005% trypsin inhibitor (Sigma; type I-S). Hepatocytes were centrifuged and washed twice in complete Hanks/HEPES buffer. Cell viability was checked microscopically by exclusion of trypan blue. Cells were finally suspended in the complete Hanks/HEPES buffer at different concentrations (10–60 mg cell dry mass/ml). Before TRS measurements, plastic bags were filled with 25 ml of those cell suspensions and stored on ice.

Once the TRS measurements were performed, 1 ml of each solution was centrifuged, and the wet pellet weight was measured. Then, after being dried overnight, the cell dry weight was measured. The cell size distribution of the hepatocytes was analyzed using a Coulter counter multichannel analyzer.

Mitochondria preparation

Rat liver mitochondria were isolated according to Johnson and Lardy (1967). The protein concentration was estimated by the biuret method using bovine serum albumin as standard. Mitochondria suspensions were made up to 5–15 mg protein/ml in the following solution: 250 mM sucrose, 0.5 mM EGTA, and 10 mM Tris-HCl (pH 7.4) supplemented with 10 mM succinate-Tris. Before TRS measurements, plastic bags were filled with 25 ml of those suspensions and stored on ice.

Determination of absorption and reduced scattering coefficients by TRS

An experimental approach, the "sample substitution method" or "matching method," has been developed in our laboratory to measure the absorption and the reduced scattering coefficients of small volume biological samples. The principle of this methods has already been detailed by Liu et al. (1993) and Beauvoit et al. (1993). Experiments were performed in a two-component system consisting of a large host medium and a small volume guest bag containing the sample.

The host medium is a solution of Intralipid (Kabi Pharmacia Inc., Clayton, NC) which looks like milk. The absorption coefficient, μ_a, can be varied by adding black ink (black India ink, No. 4416, Faber Castell Corp., Newark, NJ) to the medium (0–2 ml of ink, 5% or 20% v/v) and the scattering coefficient, μ_s', can be varied by changing the concentration of Intralipid (0.25–2% v/v). The Intralipid was placed in a 1.35-liter cylindrical container 15 cm in diameter and 8 cm high. The bottom of the guest bag was immersed ~5 cm below the surface of the host medium.

The pulsed light source and the detector of TRS were placed of 2.7–3 cm apart on opposite sides of the sample. They were both inserted into the host medium about 8–10 mm below the solution surface. Pulses were injected into the host medium by a 200-μm fiber, at a 5 MHz repetition rate, with a pulse width of 50 ps and wavelength of 780 nm. The scattered light was collected with a 3 mm diameter fiber connected to a single photon counting system. This system consists of a microchannel plate-photomultiplier tube (MCP-PMT) (Hamamatsu, R1712U) with a time resolution of 150 ps, a constant fraction discriminator (CFD), a time to amplitude converter (TAC) and a computer. Photon kinetics measured by TRS were fitted to the analytical solution for semi-infinite media (Patterson et al., 1989) with a compensation for instrument response.

Transport cross-section calculations

Mie theory

Graff et al. (1992) have shown that the calculation of the transport cross-section by the Mie theory can be approximated by the following equation:

$$\sigma_{tr} = \sigma_s(1 - g) = \pi r^2 3.28 x^{0.37}(m - 1)^{2.09}$$

where σ_s is the scattering cross-section, g is the average cosine of the scattering angle θ, x is the size parameter ($x = 2\pi r/\lambda$), m is the refractive index relative to the surrounding medium, r is the radius, and λ is the wavelength. This approximation is valid over a range of size parameter ($5 < x < 50$), of refractive index ($1 < m < 1.1$) and of g values ($g > 0.90$).

Rayleigh-Debye-Gans approximation

The transport cross-section, i.e., $\sigma_{tr} = \sigma_s(1 - g)$, can also be calculated by using the two formulas (Kerker, 1969; Graff et al., 1992):

$$\sigma_s = \frac{\lambda^2}{4\pi} \int_0^{\pi} [i_1(\theta) + i_2(\theta)] \sin\theta \, d\theta$$

$$g = \frac{\int_0^{\pi} [i_1(\theta) + i_2(\theta)] \cos\theta \sin\theta \, d\theta}{\int_0^{\pi} [i_1(\theta) + i_2(\theta)] \sin\theta \, d\theta}$$

with

$$i_1(\theta) + i_2(\theta) = x^6 \left| \frac{m^2 - 1}{m^2 + 2} \right|^2 \left\{ \frac{3}{u^3} [\sin(u) - u\cos(u)] \right\}^2 [1 + \cos^2\theta]$$

and $u = 2x \sin(\theta/2)$.

Numerical integrations were done with a total of 900 θ angles.

RESULTS

Contribution of the subcellular compartments of the liver to light scattering

The reduced scattering coefficient of a highly multiple scattering medium depends on a microscopic scattering coefficient of the constituting particles, i.e., the transport cross-section, and on two morphometric parameters: the volume of the single particle and the volume fraction occupied by the particles in the medium. Thus, the reduced scattering coefficient, μ_s', is given by the following equation:

$$\mu_s' = \frac{\sigma_{tr}}{v} \phi \qquad (1)$$

where σ_{tr} is the transport cross-section of the particle, V is the single volume, and ϕ is the volume fraction of the particles in the total volume. This equation is valid if ϕ is sufficiently small ($\phi < 0.2$). For $\phi > 0.5$, the particles are densely packed and the medium becomes almost homogeneous. In this case, the whole solution may be viewed as homogeneous medium with the scattering particles made of the inter particle space. In the limit $\phi \rightarrow 1$, the inter particle space disappears and μ_s' should approach 0. This consideration developed by Ishimaru and others for red blood cells (Reynolds et al., 1976; Ishimaru, 1978; Steinke and Shepherd, 1988) leads to the following approximate representation of μ_s':

$$\mu_s' = \frac{\sigma_{tr}}{v} \phi(1 - \phi) \qquad (2)$$

Morphometric descriptions of the normal and pathological rat liver by using electron microscopy has been performed for about three decades (Loud, 1968; Weibel et al., 1969; Blouin et al., 1977; Jakovcic et al., 1978; Furuta et al., 1992). Table 1 summarizes these quantitative stereological descriptions of the ultrastructure of the rat liver that we used for the calculations of μ_s'. The hepatocytes are by far the most prominent component of the liver parenchyma (~ 80% of the organ volume; see Table 1) while nonhepatocytes account only for about 6% of the liver volume (Blouin et al., 1977). Moreover, the mitochondrial compartment represents the most important subcellular compartment of the hepatocyte (~22% of the cell volume; see Table 1), in contrast to the other liver cells (~4% of the cell volume in endothelial or Kupffer cells; Blouin et al., 1977). The mean particle volume is ~0.7 μm^3 and the number of particles is included between 1300 and 2200. The nucleus is the second subcellular compartment regarding its volume fraction (~8%) and is the bigger compartment concerning the single volume. At last, the microbodies called also peroxisomes represent ~2% of the cell volume.

Mie theory and Rayleigh-Debye-Gans (RDG) approximation are able to calculate the transport cross-section of a scattering particle. These two mathematical models treat the scattering particle as a sphere of radius r and homogeneous relative refractive index m illuminated by an unpolarized light of wavelength λ. For our purpose, we assumed the following: 1) the liver is a mixture of three types of scattering particles randomly distributed: the whole hepatocyte, the nucleus, the mitochondria, and the peroxisomes, in regard to their respective volume fractions listed in Table 1; 2) these particles are spheres of radius r with a corresponding volume listed in Table 1; and 3) there is no interference between the different particles for light scattering, particularly between hepatocyte cytoplasm and the organelles. As the relative refractive index of the hepatocyte, the nucleus and the other

TABLE 1 Morphometric data of the rat liver and calculation of the scattering properties of the liver by the Mie theory and RDG approximation*

Structure	Volume fraction	Number density	Single volume (μm^3)	σ_{tr} (μm^2)		In vivo μ_s' (cm^{-1})	
				Mie	RDG app.	Mie	RDG app.
Hepatocyte	80.5 ± 4% of the liver	1.4×10^8 per g wet liver	5100 ± 160	7.3 ± 0.1	5.6 ± 0.1	2.2 ± 0.1	1.7 ± 0.1
Nucleus	7.6 ± 2.4% of the hepatocyte	1 per hepatocyte	345 ± 45	0.86 ± 0.06	0.75 ± 0.05	1.4 ± 0.5	1.2 ± 0.5
Mitochondria	22.6 ± 5.7% of the hepatocyte	1740 ± 462 per hepatocyte	0.67 ± 0.14	$(6.3 \pm 0.7) \times 10^{-3}$	$(5.4 \pm 0.7) \times 10^{-3}$	14.0 ± 4.5	12.1 ± 4
Peroxisomes (microbodies)	1.7 ± 0.6% of the hepatocyte	496 ± 179 per hepatocyte	0.16 ± 0.03	$(2 \pm 0.15) \times 10^{-3}$	$(1.4 \pm 0.15) \times 10^{-3}$	1.7 ± 0.7	1.2 ± 0.5

*Average electron microscopy data compiled from Loud (1968), Weibel et al. (1969), Blouin et al. (1977), Jakovcic et al. (1978). Transport cross-sections and in vivo μ_s' were calculated as described in Materials and Methods and Results, assuming a refractive index value of 1.04 relative to the extracellular medium for the hepatocyte and a value of 1.04 relative to the cytoplasm for the nucleus and the organelles.

organelles are unknown, all the computations were done within a range of refractive index already used for bacteria (Cross and Latimer, 1972), yeasts (Beauvoit et al., 1993), red blood cells (Reynolds et al., 1976), and lymphocytes (Sloot et al., 1988). Since the refractive index relative to water, measured at 633 nm for liver and for various mammalian tissues, was equal to 1.037 ± 0.007 and 1.053 ± 0.007, respectively (Bolin et al., 1989), we chose an m value for the hepatocyte equal to 1.04 relative to the extracellular medium. For the nucleus and the organelles, m was assumed to be equal to 1.04 relative to the cytoplasm, i.e., 1.08 relative to the extracellular medium (Cross and Latimer, 1972; Sloot et al., 1988; Fujime et al., 1988).

Table 1 contains the calculated transport cross-section values of the different scattering particles of the liver. Besides the fact that there is a deviation between the Mie theory and RDG approximation calculations (Table 1; Graff et al., 1992), the hepatocyte cytoplasm has a higher transport cross-section value than the nucleus, 5–7 μm^2 compared to 0.7–0.9 μm^2, for hepatocyte volume and the nucleus, respectively. The later compartment has a higher value than the organelles, 0.7–0.9 μm^2 compared to (1.4–6.3) $\times 10^{-3}$ μm^2, for the nucleus and the organelles (mitochondria and microbodies), respectively. This phenomenon illustrates the size dependence of the transport cross-section.

Finally, we have calculated the reduced scattering coefficient of the liver due to the cell volume, nucleus, mitochondria, and peroxisomes by taking into account their calculated transport cross-section values and their respective single volume and volume fraction listed in Table 1. For instance, ϕ of the mitochondria in the liver is equal to $0.226 \times 0.805 = 0.182$. Table 1 summarizes the calculated μ_s' given by the total hepatocyte volume, nucleus, mitochondria, and peroxisomes under in vivo conditions. The μ_s' values, providing from the whole cells, the nuclei and the peroxisomes, are included between 1.2 and 2.2 cm^{-1}, regardless of the mathematical model. In contrast, mitochondria compartment gives by far the largest μ_s' values, between 12 cm^{-1} and 14 cm^{-1} by using RDG and Mie models, respectively. Moreover, if the mitochondrial volume fraction inside the hepatocyte was equal to 4.5% instead of 22.6%, the calculated μ_s' due to mitochondria would be equal to ~3 cm^{-1}, a value which is close to that provided by the other compartments.

Optical properties of liver, isolated hepatocytes, and isolated mitochondria

Measurement of μ_a and μ_s' of mitochondria and hepatocyte suspensions and of the whole liver, by using TRS and a sample substitution method

The principle of the substitution method is to find the Intralipid (i.e., a standard scattering medium) and black ink (i.e., a standard absorber) concentrations at which the μ_a and μ_s' of the sample match those of the surrounding medium. One set of experimental results for a mitochondria suspension is shown in Fig. 1; the protocol remaining the same for isolated hepatocytes and for whole rat liver. The basic protocol is a two-step procedure allowing the independent determination of the μ_a and the μ_s' of the sample. The first step is the μ_a determination. TRS spectra were taken in an Intralipid solution whose absorption coefficient was gradually increased by the addition of black ink (Fig. 1 *A*). The μ_a value measured without the sample is proportional to the host ink concentration. On the other hand, the relationship between the μ_a and host ink concentration measured in the presence of the sample exhibits a "break point" (Fig. 1 *A*). At this point, the μ_a of the sample matches with that of the surrounding medium. A linear fitting to the data that deviate from those obtained without the sample can give the position of the break point and consequently the μ_a value of the mitochondria suspension. The second step is the determination of μ_s'. TRS spectra were recorded in the Intralipid solutions with different concentrations in order to increase the scattering coefficient. A relationship between μ_s' and the Intralipid concentration is shown in Fig. 1 *B*. The μ_s' value

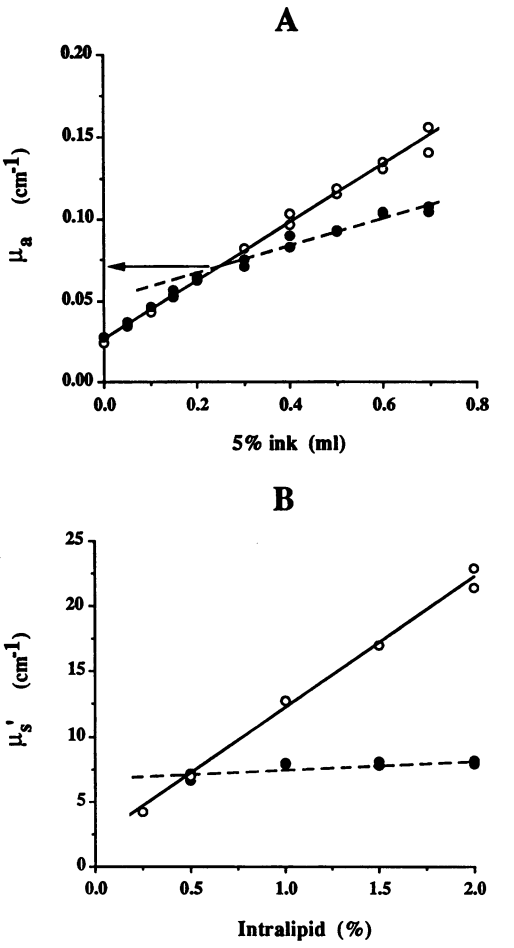

FIGURE 1 Determination of the absorption and the reduced scattering coefficients of isolated mitochondria. TRS was performed without (○) and with (●) the sample bag (12 mg protein/ml) as described in Materials and Methods. Each experimental point represents one TRS spectrum acquisition. (*A*) Example of the μ_a determination of isolated mitochondria by the substitution method. Arrow indicates the value of the μ_a corresponding to the "break point" of the dashed line. (*B*) Example of determination of the μ_s' of isolated mitochondria by the substitution method.

measured without the sample is proportional to the host Intralipid concentration (Fig. 1 *B*). In contrast, a curvilinear relationship is observed when the sample is present. At the "crossing-point" of the two lines, the μ_s' of the sample should match with that of the surrounding medium. Curve fittings of these two sets of data can give the position of the crossing-point and consequently the μ_s' value of the mitochondria suspension.

We have measured the μ_a and μ_s' of different mitochondrial suspensions by using this substitution method. As shown in Fig. 2, *A* and *B*, both μ_a and μ_s' are proportional to the mitochondrial protein concentration. The slopes of these two relationships are equal to 0.32 ± 0.05 cm²/mg protein for μ_s' (Table 2) and to (0.47 ± 0.06) × 10^{-2} cm²/mg protein for μ_a (Table 3). By the same way, we have measured the μ_a and μ_s' of isolated hepatocyte suspensions. As shown in Fig. 3, *A* and *B*, we also be found a linear relationship between both μ_a and μ_s' values and the cell dry mass concentration.The slopes of these graphs are equal to 0.079 ± 0.003 cm²/mg dry cell for μ_s' (Table 2) and to (0.18 ± 0.02) × 10^{-2} cm²/mg dry cell for μ_a (Table 3). Finally, following basically the same substitution protocol, the μ_a and μ_s' of the whole rat liver were determined. One set of experimental results for rat liver is shown in Fig. 4 *A* for the μ_a determination and in Fig. 4 *B* for the μ_s'. The experiments done on several rat livers give an average μ_s' value of ~15.9 ± 2.4 cm^{-1} (Table 2) and a mean μ_a equal to 0.53 ± 0.05 cm^{-1} (Table 3).

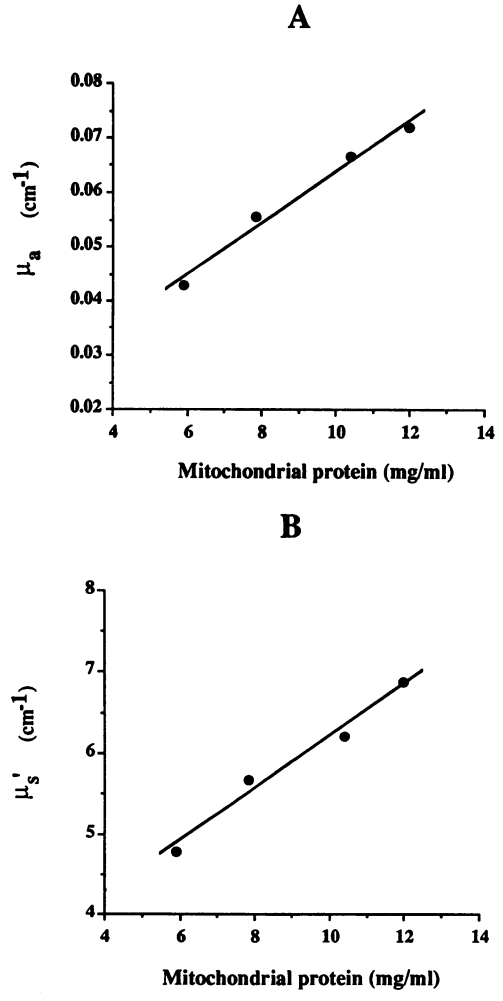

FIGURE 2 Relationship between the absorption and reduced scattering coefficients and the concentration of isolated mitochondria. The absorption (*A*) and the scattering (*B*) coefficients were determined by using TRS and the substitution method as described in Fig. 1, *A* and *B*, and in Materials and Methods.

Comparison of the optical properties of mitochondria and hepatocytes with those of the intact liver

From the slope of μ_s' and μ_a versus the mitochondrial or cell concentration, it is possible to estimate the optical properties of the liver due to the mitochondria and the hepatocytes. The extrapolations from the in vitro data to the whole tissue were done in two independent ways.

1. An estimation of the transport and absorption cross-sections was made and a subsequent calculation of the reduced scattering and absorption coefficients of the liver by using the equations developed by Ishimaru (1978) was performed. The parameters for this extrapolation are first, the number density and the single volume of isolated mitochondria and cells, and finally, the in vivo volume fractions of these particles in the liver (Tables 2 and 3).

2. A linear extrapolation of the slope of the μ_s' or μ_a versus the concentration was done by using the value of either the mitochondrial protein content or the cell dry mass content of the liver (Tables 2 and 3).

Tables 2 and 3 summarize the calculations of transport and absorption cross-sections and the extrapolations using the two procedures mentioned above. First, if we compare these two procedures, we see that the relative error on the liver μ_s' or μ_a extrapolations is higher by using the Ishimaru's formula than that obtained by using linear extrapolation (Tables 2 and 3). This can be explained by a relatively high error on both the number density and the single volume of the particles, as previously shown for yeast cells (Beauvoit et al., 1993). We can also see that both calculations from isolated mitochondria data by using Ishimaru's equations or the linear extrapolation are very close. They are respectively equal to 14.7 and 16 cm^{-1} for μ_s' (Table 2) and to 0.15 and 0.16 cm^{-1} for μ_a (Table 3). Finally, the calculations of the liver μ_a from isolated hepatocyte data are approximately the same: 0.68 and 0.47 cm^{-1}, by using Ishimaru's equation or linear extrapolation, respectively (Table 3). In contrast, the estimations of the liver μ_s' from isolated hepatocyte data were very different: 5.8 and 20.3 cm^{-1} by using the two procedures above (Table 2).

Second, the experimental transport cross-section value of the isolated mitochondria is equal to 3.7 × 10^{-3} μm^2, which is close to that computed from Mie theory or RDG approximation (Table 2). The experimental transport cross-section value of the isolated hepatocyte is equal to 15 μm^2, which

TABLE 2 Scattering properties of the rat liver and the isolated hepatocytes and mitochondria measured by TRS

Structure	$d\mu_s'/d$[mass] (cm^2 (mg proteins)$^{-1}$ or cm^2 (mg dry cell)$^{-1}$)	Theoretical σ_{tr} (μm^2)		σ_{tr} (μm^2)	Whole liver μ_s' (cm^{-1})
		Mie	RDG app.		
Liver					15.9 ± 2.4 (n = 4) 5.8 ± 1.5‡
Isolated hepatocytes	0.079 ± 0.008	6.1 ± 0.2	4.7 ± 0.3	15.1 ± 2.1*	20.3 ± 1.7§ 14.7 ± 5.5‡
Isolated mitochondria	0.32 ± 0.05	(3.4 ± 0.6) × 10^{-3}	(3.1 ± 0.6) × 10^{-3}	(3.7 ± 1.6) × 10^{-3}*	16.4 ± 2.1§

*Calculated from the following equation (Beauvoit et al., 1993): $\sigma_{tr} = (1/N)(d\mu_s'/d[\text{mass}])$ where N is the number density. $N = (8.7 \pm 2.5) \times 10^9$ mitochondria per mg mitochondrial protein (Gear and Bednarek, 1972; Schwerzmann et al., 1986) or (5.1 ± 0.5) × 10^5 cells per mg cell dry mass.
‡Calculated from the following equation (Ishimaru, 1978): $\mu_s' = (\sigma_{tr}/V)\phi(1 - \phi)$ where V is the single volume and ϕ the volume fraction. $V = 0.375 \pm 0.080$ μm^3 for isolated mitochondria (Gear and Bednarek, 1972; Schwerzmann et al., 1986) and 4114 ± 300 μm^3 for isolated hepatocytes. $\phi = 0.182 \pm 0.055$ for mitochondria and 0.805 ± 0.04 for hepatocytes in situ in the liver (Table 1).
§Calculated from the following equation: $\mu_s' = d\mu_s'/d[\text{mass}]\, M\rho$ where M is the mass ratio and ρ the density of the liver. $M = 48 \pm 5$ mg of mitochondrial proteins per g of wet liver (assuming that mitochondrial proteins account for 33% of the total proteins (see Alterations); Quinlan et al., 1983) or 242 ± 9 mg of cell dry mass per g of wet liver. ρ was assumed to be equal to 1.07 ± 0.01 g/ml (Bolender et al., 1978).

TABLE 3 Absorption properties of the rat liver and the isolated hepatocytes and mitochondria measured at 780 nm by TRS

Structure	$d\mu_a/d$[mass] × 10^2 (cm^2 (mg proteins)$^{-1}$ or cm^2 (mg dry cell)$^{-1}$)	σ_a (μm^2)	Whole liver μ_a (cm^{-1})
Liver			0.53 ± 0.05 (n = 4) 0.68 ± 0.23‡
Isolated hepatocytes	0.18 ± 0.02	0.35 ± 0.08*	0.47 ± 0.08§ 0.26 ± 0.12‡
Isolated mitochondria	0.47 ± 0.06	(5.4 ± 2.2) × 10^{-5}*	0.24 ± 0.06§

*Calculated from the following equation: $\sigma_a = (1/N)(d\mu_a/d[\text{mass}])$ where N is the number density as defined in Table 2.
‡Calculated from the following equation (Ishimaru, 1978; Steinke and Shepherd, 1988): $\mu_a = (\sigma_a/V)\phi$ where V is the single volume and ϕ the volume fraction as defined in Table 2.
§Calculated from the following equation: $\mu_a = d\mu_a/d[\text{mass}]\, M\rho$ where M is the mass ratio and ρ the density of the liver, which the respective values are the same than in Table 2.

value is 2.4 and 3.2 times higher than that computed from Mie theory and RDG approximation, respectively (Table 2).

Finally, the comparison between the in vitro to in vivo extrapolations and the whole rat liver measurements leads to the following conclusions. The reduced scattering coefficient of the liver is close to that estimated from isolated mitochondria: 15.9 cm^{-1} vs. 14.7–16.4 cm^{-1} (Table 2). Moreover, the μ_s' measured for the liver is included between the calculations provided by isolated hepatocyte measurements: 15.9 cm^{-1} vs. 5.8–20.3 cm^{-1} (Table 2). The absorption coefficient of the liver is twofold higher than that estimated from the isolated mitochondria measurements: 0.53 cm^{-1} vs. 0.24–0.26 cm^{-1} (Table 3). However, the μ_a value of the whole liver fits quite well with those extrapolated from isolated hepatocyte measurements 0.53 cm^{-1} vs. 0.47–0.68 cm^{-1} (Table 3).

DISCUSSION

The rat liver organ offers a unique opportunity to investigate the contribution of the mitochondria to the optical properties of the whole liver, since we are able to isolate a quite homogeneous population of hepatocyte and mitochondria without significant damage of the cell and mitochondria architecture and composition. In this study, we used the time-resolved spectroscopy and a sample substitution method to quantitate the absorption and reduced scattering coefficients of rat livers and of hepatocyte or mitochondria suspensions. This method has been successfully used in the laboratory to measure μ_a and μ_s' of small biological samples such as human finger (H. Liu and and B. Chance, personal communication) and yeast cell suspensions (Beauvoit et al., 1993).

Origin of the light absorption of the liver at 780 nm

Our TRS measurements of the absorption coefficient of the blood-free liver gave an average value of ~0.53 cm^{-1}. This value is close to that extrapolated from in vitro measurements done on isolated hepatocyte suspensions (Table 3). However, the whole liver μ_a value is about twice higher than that extrapolated from in vitro measurements performed on isolated mitochondria suspensions (Table 3). Thus the liver contains NIR absorbers other than the mitochondrial cytochrome aa_3, which is assumed to be the main cellular chromophore in blood-free organs between 750 and 900 nm. The explanation

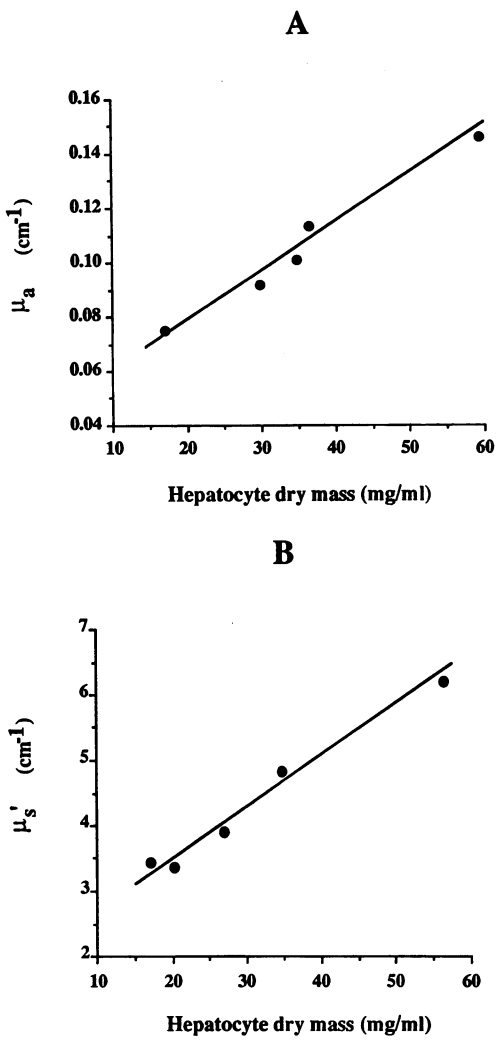

FIGURE 3 Relationship between the absorption and reduced scattering coefficients and the concentration of isolated hepatocytes. The absorption (*A*) and the scattering (*B*) coefficients were determined by using TRS and the substitution method as described in Materials and Methods.

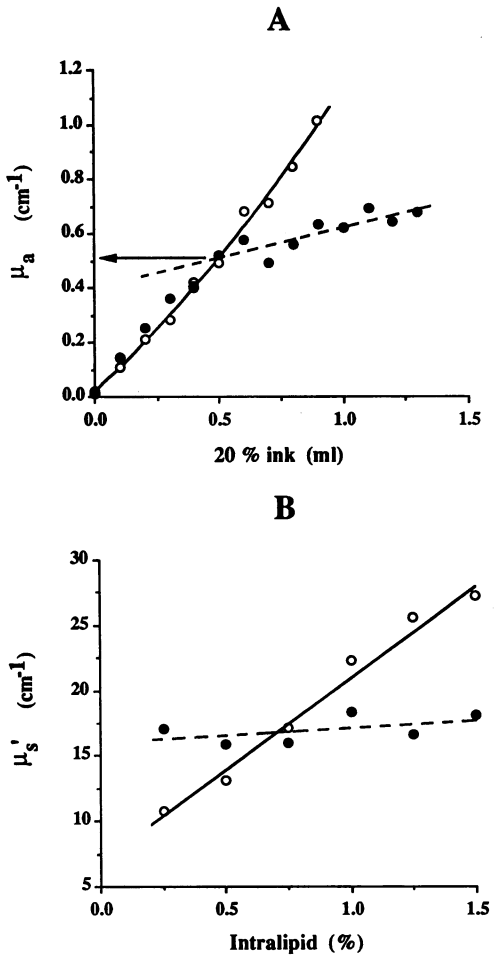

FIGURE 4 Determination of the absorption and the reduced scattering coefficients of blood-free rat liver. TRS was performed without (○) and with (●) the sample bag containing two blood-free rat livers (10 g wet mass) as described in Materials and Methods. Each experimental point is the average of four TRS spectrum acquisitions. (*A*) Example of the μ_a determination of rat liver by the substitution method. Arrow indicates the value of the μ_a corresponding to the "break point" of the dashed line. (*B*) Example of determination of the μ_s' of rat liver by the substitution method.

of this discrepancy is not the goal of this paper but, as discussed in previous reports (Paigen, 1956; Sato et al., 1981; Miyake et al., 1991), the possibility of remnant hemoglobin must be considered, as well as the presence of cytosolic chromophores such as the Cu/Zn superoxide dismutase (Carrico and Deutsh, 1969).

Origin of the light scattering of the liver

Light propagation in biological materials is dominated by scattering, i.e., the reduced albedo $c' = \mu_s'/(\mu_s' + \mu_a)$ is close to 1, because of the inhomogeneities of both the cellular structure, composition and particle size. In a tissue, the major scattering media and particles are the extracellular spaces, the cellular space, the intracellular nucleus, and organelles. As shown by the morphometric data of the liver, each constituting particle of the liver has its own characteristic size, shape, and volume fraction (Table 1; Loud, 1968; Weibel et al., 1969; Blouin et al., 1977; Jakovcic et al., 1978).

Theoretical analysis of the scattering properties of the rat liver

Several mathematical models lead to the calculation of the microscopic parameter of the scattering particles, i.e., the transport cross-section, assuming they are spherical and have an homogeneous refractive index. Mie theory and RDG approximation, either alone or combined, has been often used to model scattering in biological samples, for instance in secretory granules (Fujime et al., 1988), mitochondria (Frank et al., 1989), bacteria (Cross and Latimer, 1972), yeasts (Beauvoit et al., 1993), red blood cells (Reynolds et al., 1976; Steinke and Shepherd, 1988), and lymphocytes (Sloot et al., 1988). In this report, by using these two models, we have calculated the transport cross-section of the liver cell, the nucleus, and the major organelles of mitochondria and peroxisomes. In spite of a 10–20% deviation between the values from Mie theory and RDG, we have confirmed that the σ_{tr}

value depends on the size of the particle: the liver cell has the highest σ_{tr} value and the peroxisome has the smallest (Table 1). Moreover, we have calculated the macroscopic scattering coefficient provided respectively by the whole cell volume, the nucleus, the mitochondria, and the peroxisomes under in vivo conditions. This can be done by using the Ishimaru's equation (see Eq. 2 and Ishimaru, 1978) giving the μ_s' as a function of the single volume of the particle and its volume fraction inside the liver, in respect to the liver morphometric data of Table 1. Surprisingly, we have found that the mitochondria population in liver provides the most important scattering coefficient, in contrast to the total cell volume, the nucleus, and the microbodies (Table 1). This result can be explained by a combination of a small single volume value of the mitochondria and a high volume fraction of the mitochondrial compartment inside the liver. Then, if the mitochondrial volume fraction changed from 22.6 to 4.5%, a value close to that of the nonhepatocyte liver cells (Blouin et al., 1977), the calculated μ_s' value provided by the mitochondria compartment would become comparable to that calculating from the other liver components.

The theoretical analysis above presupposes some assumptions, namely, 1) the liver is a randomly distributed mixture of scattering particles; 2) the particles are spherical and have a homogeneous refractive index; and 3) there is no interference between the scattering of the different particles, and especially between the intracellular organelles and the whole cell. The first assumptions seems reasonable since: the hepatocyte is the most prominent component of the liver parenchyma (Blouin et al., 1977), the heterogeneity of cells and organelles in the liver, i.e., periportal versus perivenous, is taken into account in the morphometric data of Table 1, and a polydisperse morphology of the mitochondrial compartment has been shown by fluorescent staining (Lemasters et al., 1987; Reber et al., 1990) and electron microscopy (Loud, 1968; Weibel et al., 1969; Blouin et al., 1977; Jakovcic et al., 1978) of the rat hepatocytes. Nevertheless, the main simplifications borne by our mathematical treatment are that the exact value of the refractive index of each liver component is unknown, organelles are interacting with each other in a complex membrane network, and cells and organelles are not exactly spherical (Furuta et al., 1992). The existence of those assumptions in mathematical models warns careful readers not to take the calculated μ_s' values of the liver per se but as indicators of a tendency.

We have quantitated the reduced scattering coefficient of the liver and compared with that calculated from in vitro data on isolated mitochondria and cell. As for the absorption coefficient, we used two extrapolation procedures: a linear extrapolation using directly the slope of the in vitro μ_s' versus the cell or mitochondria concentration and a nonlinear extrapolation using the transport cross-section calculation of the mitochondria and the hepatocyte and then using Eq. 2.

Scattering properties of the hepatocyte

From the in vitro experiments, we have calculated a liver μ_s' of ~6–20 cm^{-1} depending on the calculation procedure (Table 2). Of importance is the fact that the μ_s' measured on the whole liver is equal to ~16 cm^{-1}, which value is included between the previously extrapolated ones (Table 2). The deviation between the two extrapolation procedures comes from the complexity of the scattering events in the cell suspensions. Thus, light scattering is both due to the whole hepatocyte volume and to the intracellular organelles, encompassing mitochondria. Both of these calculation procedures fail to fully describe these two phenomena. As a matter of fact, the linear extrapolation gives an overestimation of μ_s', since it does not consider an attenuation of the light scattering by the in vivo high cell density (Ishimaru, 1978). In contrast, Eq. 2 provides an underestimation of μ_s' since it takes into account the light attenuation when the cell density is high ($\phi > 0.5$) but excludes the scattering due to the particles inside the hepatocyte (Ishimaru, 1978). Indeed, when $\phi \rightarrow 1$, μ_s' becomes close to 0 regardless to the light scattering due to the mitochondria inside the cell.

The experimental transport cross-section of the hepatocyte is about 2 to 3 times higher than that computed from Mie theory or RDG approximation (Table 2). Such a discrepancy can either be explained by the sensitivity of the models toward the refractive index or by a misestimation of the cellular anisotropic factor (i.e., $1 - g$ value) by the mathematical models, as already pointed out for red blood cells (Steinke and Shepherd, 1988). This observation is not in accordance with the results obtained on yeast cells, where the experimental values fitted well with the calculated ones, suggesting that the cell volume was the primary factor affecting the light scattering of yeast cell (Beauvoit et al., 1993).

Scattering properties of the mitochondria

The experimental transport cross-section value of the isolated mitochondria is close to that calculated by Mie and RDG models (Table 2). Besides the careful reading of these theoretical calculations, this result strongly suggests that, in contrast to the whole cell, the mitochondria can be approximated to a homogeneous spherical particle for the light scattering. From the in vitro experiments on isolated mitochondria, we have calculated a liver μ_s' of about 14 to 16 cm^{-1} depending on the calculation procedure (Table 2). The most important observation is that the measurements on the whole liver fit very well with the in vitro to in vivo extrapolations. However, such a comparison supposes that isolated mitochondria in aqueous solution are structurally in the same conformation than in situ in the liver. Nevertheless, the significant point is that isolated mitochondria in the presence of a respiratory substrate and without ADP (state 4) display an "orthodox" conformation as is usually observed after fixation within intact tissue (Hackenbrock, 1966). As predicted by our preliminary theoretical study, these quantitative results confirm the crucial role of the mitochondria to determine the scattering properties of the liver.

To summarize, our preliminary theoretical approach, based on the morphometric data of the liver, has shown that the mitochondria compartment could be the primary factor determining the reduced scattering coefficient of the rat liver.

Our quantitation of the absorption and scattering properties of isolated hepatocytes and mitochondria and the subsequent in vitro to in vivo extrapolations have demonstrated that the mitochondria provide only 50% of the liver organ absorption coefficient at 780 nm and under our experimental conditions, and that the origin of the liver light scattering lies totally in its mitochondria content. This phenomenon might be related to two structural and metabolic properties of the liver, namely, a high volume fraction and a polydisperse morphology of the mitochondrial compartment in the hepatocyte.

This work was supported in part by National Institutes of Health grant CA50766.

REFERENCES

Beauvoit, B., H. Liu, K. Kang, P. D. Kaplan, M. Miwa, and B. Chance. 1993. Characterization of absorption and scattering properties for various yeast strains by time-resolved spectroscopy. *Cell Biophys.* 23:1–16.

Berry, M. N., A. M. Edwards, G. J. Barrit, M. B. Grivell, H. J. Halls, B. J. Gannon, and D. S. Friend. 1991. Isolated hepatocytes. Preparation, properties and applications. *In* Laboratory Techniques in Biochemistry and Molecular Biology, Vol. 21. R. H. Burdon and P. H. Knippenberg, editors. Elsevier, New York.

Blouin, A., R. P. Bolender, and E. R. Weibel. 1977. Distribution of organelles and membranes between hepatocytes and nonhepatocytes in the rat liver parenchyma. A stereological study. *J. Cell Biol.* 72:441–455.

Bohren C. V., and D. R. Huffman. 1983. Absorption and Scattering of Light by Small Particles. John Wiley and Sons, New York.

Bolender, R. P., D. Paumgartner, G. Losa, D. Muellener, and E. R. Weibel. 1978. Integrated stereological and biochemical studies on hepatocytic membranes. I. Membrane recoveries in subcellular fractions. *J. Cell Biol.* 77:565–583.

Bolin, F. P., L. E. Preuss, R. C. Taylor, and R. J. Ference. 1989. Refractive index of some mammalian tissues using a fiber optic cladding method. *Appl. Opt.* 28: 2297–2303.

Carrico, R. J., and H. F. Deutsch. 1969. Isolation of human hepatocuprein and cerebrocuprein. Their identity with erythrocuprein. *J. Biol. Chem.* 244:6087–6093.

Chance, B., J. Leigh, H. Miyake, D. Smith, S. Nioka, R. Greenfeld, M. Finlander, K. Kaufmann, W. Levy, M. Young, P. Cohen, H. Yoshioka, and R. Boretsky. 1988a. Comparison of time-resolved and un-resolved measurements of deoxyhemoglobin in brain. *Proc. Natl. Acad. Sci. USA.* 85:4971–4975.

Chance, B., S. Nioka, J. Kent, K. Mc Cully, M. Fountain, R. Greenfeld, and G. Holtom. 1988b. Time-resolved spectroscopy of hemoglobin and myoglobin resting and ischemic muscle. *Anal. Biochem.* 174:698–707.

Chen, L. B. 1989. Fluorescent labeling of mitochondria. *Methods Cell Biol.* 29:103–123.

Cross, D. A., and P. Latimer. 1972. Angular dependence of scattering from *Escherichia coli* cells. *Appl. Opt.* 11: 1225–1228.

David, H., W. Krause, and D. Behrisch. 1990. Morphometric characterization of isolated hepatocytes. *Biomed. Biophys. Acta.* 49:563–571.

Frank, K. H., M. Kessler, K. Appelbaum, H. P. Albrecht, and E. D. Mauch. 1989. Measurements of angular distributions of Rayleigh and Mie scattering events in biological models. *Phys. Med. Biol.* 34:1901–1916.

Fujime, S., M. Takasaki-Ohsita, and S. Miyamoto. 1988. Dynamic light scattering from polydisperse suspensions of large spheres. Characterization of isolated secretory granules. *Biophys. J.* 54:1179–1184.

Furuta, K., S. Ohno, Y. Gibo, K. Kiyosawa, and S. Furuta. 1992. Three-dimensional ultrastructure of normal rat hepatocytes by quick-freezing and deep-etching method. *J. Gastroenterol. Hepatol.* 7:486–490.

Gear, A. R. L., and J. M. Bednarek. 1972. Direct counting and sizing of mitochondria in solution. *J. Cell Biol.* 54:325–345.

Graaff, R., J. G. Aarnoudse, J. R. Zijp, P. M. A. Sloot, F. F. M. de Mul, J. Greve, and M. H. Koelink. 1992. Reduced light-scattering properties for mixtures of spherical particles: a simple approximation derived from Mie calculation. *Appl. Opt.* 31:1370–1376.

Hackenbrok, C. R. 1966. Ultrastructural bases for metabolically linked mechanical activity in mitochondria. I. Reversible ultrastructural changes with change in metabolic steady state in isolated liver mitochondria. *J. Cell Biol.* 30:269–297.

Halestrap, A. P. 1989. The regulation of the matrix volume of mammalian mitochondria in vivo and in vitro and its role in the control of mitochondrial metabolism. *Biochim. Biophys. Acta.* 973:355–382.

Hoffmann, H. P., and C. Avers. 1973. Mitochondrion of yeast: ultrastructural evidence for one giant, branched organelle per cell. *Nature.* 181: 749–751.

Ishimaru, A. 1978. Wave Propagation and Scattering in Random Media. Academic Press, New York.

Jakovcic, S., H. H. Swift, N. J. Gross, and M. Rabinowitz. 1978. Biochemical and stereological analysis of rat liver mitochondria in different thyroid states. *J. Cell Biol.* 77:887–901.

Johnson, D., and H. Lardy. 1967. Isolation of liver or kidney mitochondria. *Methods Enzymol.* 10:94–96.

Johnson, L. V., M. L. Walsh, and L. B. Chen. 1980. Localization of mitochondria in living cells with rhodamine 123. *Proc. Natl. Acad. Sci. USA.* 77:990–994.

Kerker, M. 1969. The Scattering of Light, and Other Electromagnetic Radiation. Academic Press, New York.

Lemasters, J. J., J. Di Guiseppi, A. L. Nieminen, and B. Herman. 1987. Blebbing, free Ca^{2+} and mitochondrial membrane potential preceding cell death in hepatocytes. *Nature.* 325:78–81.

Liu, H., M. Miwa, B. Beauvoit, N. G. Wang, and B. Chance. 1993. Characterization of absorption and scattering properties of small-volume biological samples using time-resolved spectroscopy. *Anal. Biochem.* 213: 378–385.

Lloyd, D. 1974. The Mitochondria of Microorganisms. Academic Press, New York.

Loud, A. V. 1968. A quantitative stereological description of the ultrastructure of normal rat liver parenchymal cell. *J. Cell Biol.* 37:27–39.

Miyakawa, I., H. Aoi, N. Sando, and T. Kuroiwa. 1984. Fluorescence microscopic studies of mitochondrial nucleoids during meiosis and sporulation in the yeast, *Saccharomyces cerevisiae*. *J. Cell. Sci.* 66: 21–38.

Miyake, H., S. Nioka, A. Zaman, D. S. Smith, and B. Chance. 1991. The detection of cytochrome oxidase heme iron and copper absorption in the blood-perfused and blood-free brain in normoxia and hypoxia. *Anal. Biochem.* 192:149–155.

Paigen, K. 1956. Hemoglobin as the red pigment of microsomes. *Biochim. Biophys. Acta.* 19:297–299.

Patterson, M. S., B. Chance, and B. C. Wilson. 1989. Time resolved reflectance and transmittance for the noninvasive measurement of tissue optical properties. *Appl. Opt.* 28:2331–2336.

Pfaller, W., C. Willinger, B. Stoll, C. Hallbrucker, F. Lang, and D. Haussinger. 1993. Structural reaction pattern of hepatocytes following exposure to hypotonicity. *J. Cell. Physiol.* 154:248–253.

Quinlan, P. T., A. P. Thomas, A. E. Armston, and A. P. Halestrap. 1983. Measurement of the mitochondrial volume in hepatocytes without cell disruption and its elevation by hormones and valinomycin. *Biochem. J.* 214:395–404.

Reber, B. F. X ., R. Somogyi, and J. W. Stucki. 1990. Hormone-induced intracellular calcium oscillations and mitochondrial energy supply in single hepatocytes. *Biochim. Biophys. Acta.* 1018:190–193.

Reynolds, L., C. Johnson, and A. Ishimaru. 1976. Diffusive reflectance from a finite blood medium: to the modelling of fiber optic catheters. *Appl. Opt.* 15:2059–2067.

Sato, N., T. Matsumura, M. Shichiri, T. Kamada, H. Abe, and B. Hagihara. 1981. Hemoperfusion, rate of oxygen consumption and redox levels of mitochondrial cytochrome c (+ c1) in liver in situ of anesthetized rat measured by reflectance spectrophotometry. *Biochim. Biophys. Acta.* 634:1–10.

Schwerzmann, K., L. M. Cruz-Orive, R. Eggman, A. Sanger, and E. R. Weibel. 1986. Molecular architecture of the inner membrane of mitochondria from rat liver: a combined biochemical and stereological study. *J. Cell Biol.* 102:97–103.

Sevick, E. M., B. Chance, J. Leigh, S. Nioka, and M. Maris. 1991. Quantitation of time- and frequency-resolved optical spectra for the determination of tissue oxygenation. *Anal. Biochem.* 195:330–351.

Sloot, P. M. A., A. G. Hoekstra, and C. G. Figdor. 1988. Osmotic response of lymphocytes measured by means of forward light scattering: theoretical considerations. *Cytometry*. 9:636–641.

Smiley, S. T., M. Reers, C. Mottola-Hartshorn, M. Lin, A. Chen, T. W. Smith, G. D. Steele, and L. B. Chen. 1991. Intracellular heterogeneity in mitochondrial membrane potentials revealed by a J-aggregate-forming lipophilic cation JC-1. *Proc. Natl. Acad. Sci. USA*. 88: 3671–3675.

Steinke, J. M., and Shepherd, A. P. 1988. Comparison of Mie theory and the light scattering of red blood cells. *Appl. Opt.* 27:4027–4033

Stevens, B. 1981. Mitochondrial structure. *In* The Molecular Biology of the Yeast *Saccharomyces cerevisiae*. Life Cycle and Inheritance. J. N. Strathern, E. W. Jones, and J. R. Broach, editors. Cold Spring Harbor Laboratory, Cold Spring Harbor, New York. 471–504.

Tandler, B., and C. L. Hoppel. 1986. Studies on giant mitochondria. *Ann. N. Y. Acad. Sci.* 488:65–81.

Van de Hulst, H. C. 1957. Light Scattering by Small Particles. John Wiley and Sons, New York.

Weibel, E. R., W. Staubli, H. R. Gnagi, and F. A. Hess. 1969. Correlated morphometric and biochemical studies on the liver cell. I. Morphometric model, stereologic methods, and normal morphometric data for rat liver. *J. Cell Biol.* 42:68–84.

Wilson, B. C., E. Sevick, M. S. Patterson, and B. Chance. 1992. Time-dependent optical spectroscopy and imaging for biomedical applications. *Proc. IEEE*. 80:918–930.